ISAS - INTERNATIONAL SCHOOL FOR ADVANCED STUDIES

Reconstruction and Faceting at the surface of noble metals: Au(100) and its vicinals

Thesis submitted for the degree of

"Magister Philosophiæ"

CANDIDATE

Daniele Passerone

SUPERVISORS

Dr. Furio Ercolessi

Prof. Erio Tosatti

October 1995

SISSA - SCUOLA INTERNAZIONALE SUPERIORE STUDI AVANZATI

TRIESTE

Strada Costiera 11

TRIESTE

SISSA ISAS
SCUOLA INTERNAZIONALE SUPERIORE DI STUDI AVANZATI
INTERNATIONAL SCHOOL FOR ADVANCED STUDIES

Reconstruction and Faceting at the surface of noble metals: Au(100) and its vicinals

Thesis submitted for the degree of

"Magister Philosophiæ"

CANDIDATE

Daniele Passerone

SUPERVISORS

Dr. Furio Ercolessi

Prof. Erio Tosatti

October 1995

Table of Contents

1 Introduction

1.1 What is faceting ?

The free energy of a crystal surface depends on its orientation. This simple fact has a deep influence on the thermodynamic stability of different orientations. As discussed in the seminal works of Wulff [1] and Herring [2], some orientations are unstable and do not appear in the equilibrium shape of a finite crystal. An initially flat, indefinitely extende surface with an unstable orientation would then evolve towards a so-called *hill and valley structure, i.e.* a situation in which the overall orientation of the surface is maintained. but the surface is broken into macroscopic zones with two coexisting different orientations: this is called *faceting.* For example, one orientation could be represented by a flat, high-symmetry oriented facet, the other by a stepped, tilted vicinal surface of the former one.

Faceting may occur because the minimum free energy condition may not correspond to a minimum area structure. The system will increase its overall exposed area if this is energetically convenient. This occurs when the following conditions are satisfied:

$$A_0\vec{n}_0 = A_a\vec{n}_a + A_b\vec{n}_b \tag{1.1}$$

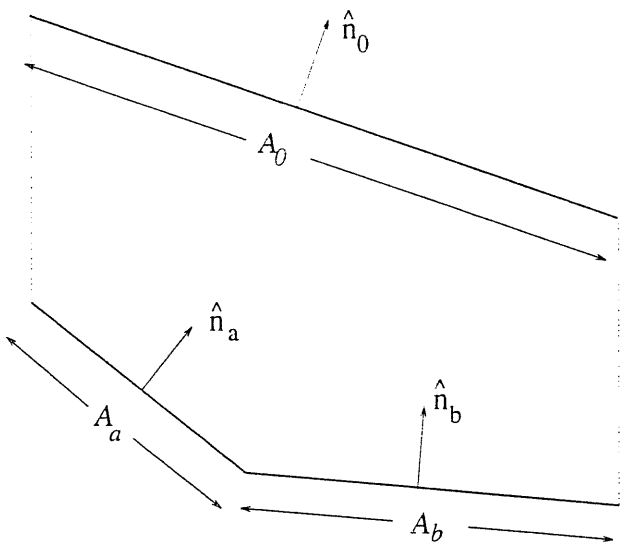

Figure 1.1: A flat surface versus a faceted one: the areas of the differently oriented zones are indicated.

$$A_0\gamma(\vec{n}_0) \quad > \quad A_a\gamma(\vec{n}_a) + A_b\gamma(\vec{n}_b). \tag{1.2}$$

All the symbols are defined by Fig.1.1. The pair of conditions (1.1) and (1.2) tells us that faceting is a first-order phase separation.

First order phase separations generally correspond to situations of non-convexity of the overall free energy of the system. The relevant Helmholtz free energy to be minimized in our problem is the surface free energy (per unit area) $\gamma(\theta, T)$ multiplied by the total area. Introducing a reference orientation $\theta = 0$ and referring to units of *projected* areas, the quantity to minimize is $\frac{\gamma(\theta,T)}{\cos(\theta)}$. $\theta = 0$ usually corresponds to a flat crystal surface with low Miller indexes.

To understand in a naïve way how faceting could occur in practice, let us expand $\frac{\gamma(\theta,T)}{\cos(\theta)}$ in powers of $|\tan(\theta)|$:

$$\frac{\gamma(\theta,T)}{\cos(\theta)} = \sigma_0(T) + \frac{\beta(T)}{h}|\tan\theta| + g(T)|\tan\theta|^3. \qquad (1.3)$$

The zeroth order term of the expansion is the surface free energy of the flat surface, $\sigma_0(T)$. The linear term is the energy cost per unit length of a step, $\beta(T)$, times the step density for steps of height h ($\tan\theta = \frac{h}{L}$, where L is the width of a terrace).

The higher-order terms stem by the effective interaction between the steps; the second order term is zero due to overall charge neutrality (no interaction of order L^{-1} is present), whereas the third order term includes all the interactions with a potential behaving like L^{-2}. Interactions between steps can be of various origin: entropic, dipolar, surface stress. The first ones arise from the fluctuations and from the non-overlapping condition of the steps, the second ones from the interactions between dipoles formed by the particular arrangement of atoms near the steps, and the stress induced interactions from the perturbing effect of the step on the surface stress field [3]. All these interactions, albeit of very different origin, show the same behaviour in the potential: $V \equiv L^{-2}$, so their effects can be all incorporated in the $g(T)$ factor in (1.3). We neglect fourth or higher order terms.

Let us now suppose that the surface of a crystal could 'choose' between a phase with high step formation energy and low energy of the terraces (favourable at low tilting angles), and another phase with a lower step formation energy but higher terrace energy, which is favoured at high step density; the envelope of the two phases can lead in this case to a concave form for the free energy density curve (see Fig.1.2). If the overall orientation of the surface ranges between $\theta = 0$ and $\theta = \theta_f$, the condition (1.2) (*i.e.* a Maxwell construction)

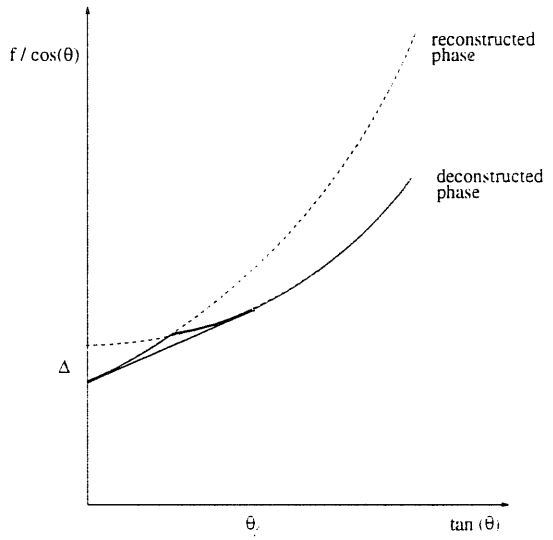

Figure 1.2: Two free energy curves corresponding to different phases of the surface; the envelope is concave and the faceting separation occurs, with the angle θ_f determined by the Maxwell construction.

is verified and corresponds to faceting between $\theta = 0$ and $\theta = \theta_f$. Macroscopic faceting may occur via several mechanisms: for example, the adsorption of O_2 induces faceting of stepped Ag(110) [4] (in this case the two phases among which the surface has to choose are the clean and the adsorbed one); it has been hypothesized that the faceting transformation of stepped Si(113) at 1220 K occurs by virtue of a direct attraction between steps [5] (in this case the overall free energy would be concave due to this attractive interaction); surface melting induces phase separation between molten and non-molten surfaces of stepped Pb(111)[6].

The case of 'magic vicinals' is yet another interesting one: magic vicinals are stepped surfaces whose orientation lies near a facet (flat) orientation: they are stabilized by the near commensurability between the step separation and the reconstruction period. Such

surfaces were originally predicted for Au(001)[7], and have been observed experimentally for Pt(001) [8] and for Au(100) [9, 10]. Last but not least (it is the motivation for our work), faceting may be induced by surface reconstruction. The uniformly stepped surface is in this case replaced by coexistence among reconstructed facets and unreconstructed, stepped regions: the free energy cost of a step is larger on the reconstructed surface than on the unreconstructed surface. This kind of faceting has been observed in Si(111)[11], induced by the (7×7) reconstruction; in Pt(001) [8] and in Au(100) [9], induced by the hexagonal reconstruction (see section 3.1). In Fig.1.3 we observe the experimental phase diagram for Au(100). The flat surface undergoes a first order phase transition from hexagonal to unreconstructed at 1153 K. A surface miscut towards the (110) direction by 1.4° is stable at high temperatures and undergoes a faceting phase separation with a faceting angle which varies with temperature. To understand phenomenologically the variation of the faceting angle, one can consider again the expression (1.3) for the free energy and apply it both to the reconstructed and to the unreconstructed phase, assuming a reconstruction energy Δ:

$$\frac{\gamma_R}{\cos\theta} = \sigma_{0R} + \frac{\beta_R}{h}|\tan\theta| + g_R|\tan\theta|^3 \tag{1.4}$$

$$\frac{\gamma_U}{\cos\theta} = \sigma_{0R} + \Delta + \frac{\beta_U}{h}|\tan\theta| + g_U|\tan\theta|^3, \tag{1.5}$$

where $\beta_R > \beta_U$; the Maxwell construction, *i.e.* the condition for phase separation leads to the following expression for the faceting angle:

$$|\tan\theta_F| = |\frac{\Delta}{2g_D}|^{\frac{1}{3}}. \tag{1.6}$$

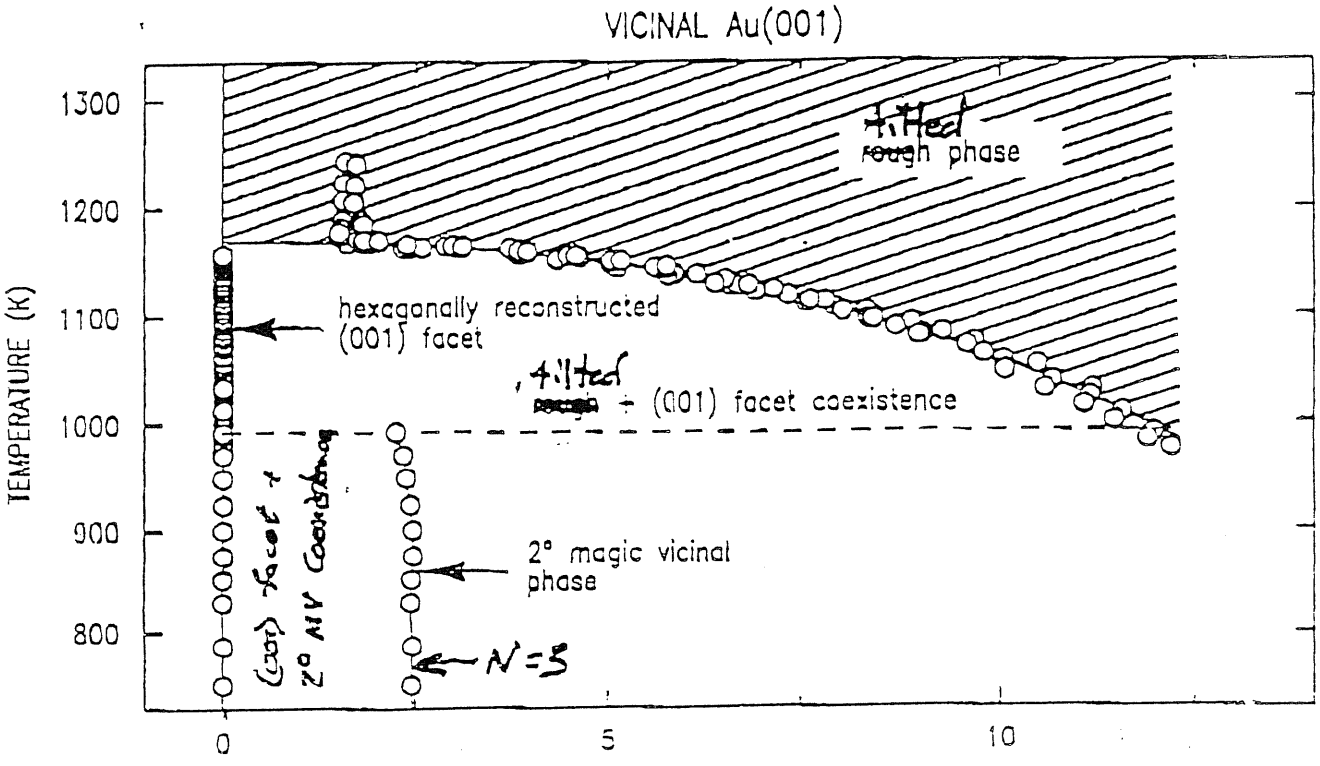

Figure 1.3: The experimental phase diagram for Pt [8] and for Au [9].

Near the deconstruction temperature T_D, Δ goes to zero linearly with $(T_D - T)$ and a good agreement with the experimental phase diagram is obtained.

At a more microscopic level, reconstruction-induced faceting is still largely to be understood. In the following chapters, we shall present theoretical models and computer simulations aiming at investigating the physics of reconstructed surfaces.

2 Lipowsky's approach

The presence of a step on a flat surface can induce several effects both on the structure and on the thermodynamic behaviour of the surface itself. A possible phenomenological mechanism to explain the complex orientational phase diagram of reconstructed surfaces has been already identified (see section 1.1): the energy cost associated to the formation of a step on a reconstructed surface is higher than the cost related to the formation of the same step on a non-reconstructed face. This picture, although simple and intuitive , cannot answer to some fundamental questions: what is the free energy of the surface? how does the presence of steps influence the local surface structure and how can this presence lead to faceting between reconstructed, flat terraces and non-reconstructed, tilted zones?

An alternative approach to this problem is to consider the analogy with a problem of *surface wetting.* In a typical surface wetting scenario one considers a system at the coexistence of two phases (*i.e.* solid and vapour), with a layer of the third phase (*i.e.* liquid) appearing at the interface.

The first step towards the understanding of such situation is to consider a d-dimensional semi-infinite system with a (d-1)-dimensional free surface. The coordinate perpendicular to

the surface is denoted by z, whereas the *d-1* Cartesian coordinates parallel to the surface are denoted by x. The system is described by a scalar order parameter with a Landau free-energy functional of the general form:

$$F[\Phi] = \int d^{d-1}x \int dz [\frac{1}{2}(\vec{\nabla}\Phi)^2 + f(\Phi) + \delta(z) f_1(\Phi)] \tag{2.1}$$

for the scalar field $\Phi(x,z)$. z is the coordinate perpendicular to the $(d-1)$-dimensional surface and

$$f(\Phi) = \frac{1}{2}a\Phi^2 - \frac{1}{3}b\Phi^3 + \frac{1}{4}c\Phi^4 \tag{2.2}$$

$$f_1(\Phi) = -h_1\Phi + a_1\Phi^2. \tag{2.3}$$

The bulk properties of this model are governed by the term $f(\Phi)$, and the bulk order is described by the order parameter $\Phi = M_B$ which corresponds to the global minimum of $f(\Phi)$. Positive coefficients $a, b. c$ within eq.(2.2) lead to a first-order bulk transition.

At the transition temperature $T = T^*$. the disordered state with $\Phi = 0$ and the ordered state with $\Phi = M_B^* > 0$ coexist.

Since the translational invariance is broken by the free surface, the order parameter $M = \langle\Phi\rangle$ depends on the distance from the surface. Thus the mean field states of the semi-infinite system may be described in terms of the order-parameter profiles $M(z)$.

Within Landau theory, these profiles are obtained from the variational principle $\frac{\delta F[\Phi]}{\delta\Phi} = 0$ with $\Phi(x,z) = M(z)$. This leads to a classical motion equation [12] with a boundary condition at the surface and another boundary condition at $z \to \infty$, *i.e.* $M(z)$ must approach the value M_B of the order parameter in the bulk. Solving the motion equation

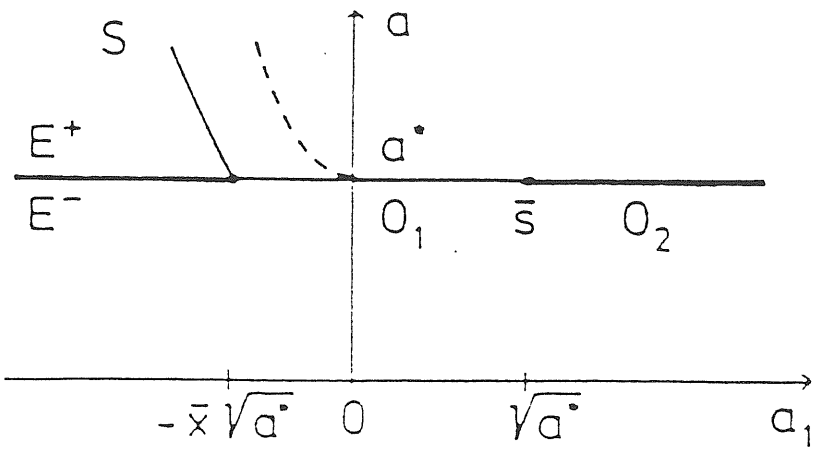

Figure 2.1: Global (a, a_1) phase diagram.

in this case leads to a global (a, a_1) phase diagram (fig.2.1). $a = a^*$ corresponds to the bulk transition temperature $T = T^*$. Different kinds of phase transitions are present, corresponding to various physical situations like surface-induced ordering (SIO) and surface-induced disordering (SID). In our case we are interested in the line O_2 which leads to a profile $M(z)$ of the kind depicted in fig.2.2. This is the 'Surface-Induced Disordering' case. The order parameter develops an interface at $z =< l >$. It is interesting to exploit the behaviour of this interface; in MF theory this length shows a logarithmically divergent behaviour. MF theory neglects fluctuations in the local position of the interface. A first improvement can be obtained if one introduces a collective coordinate ζ describing the interface:

$$\Phi(x, z) = M(z - \zeta(x)). \tag{2.4}$$

If (2.4) is inserted into (2.1), a straightforward calculation leads to a renormalized interaction term of exponential form, and a field-theoretical model in $d - 1$ dimensions has to be solved. The MF theory for this model leads to the same critical properties at the

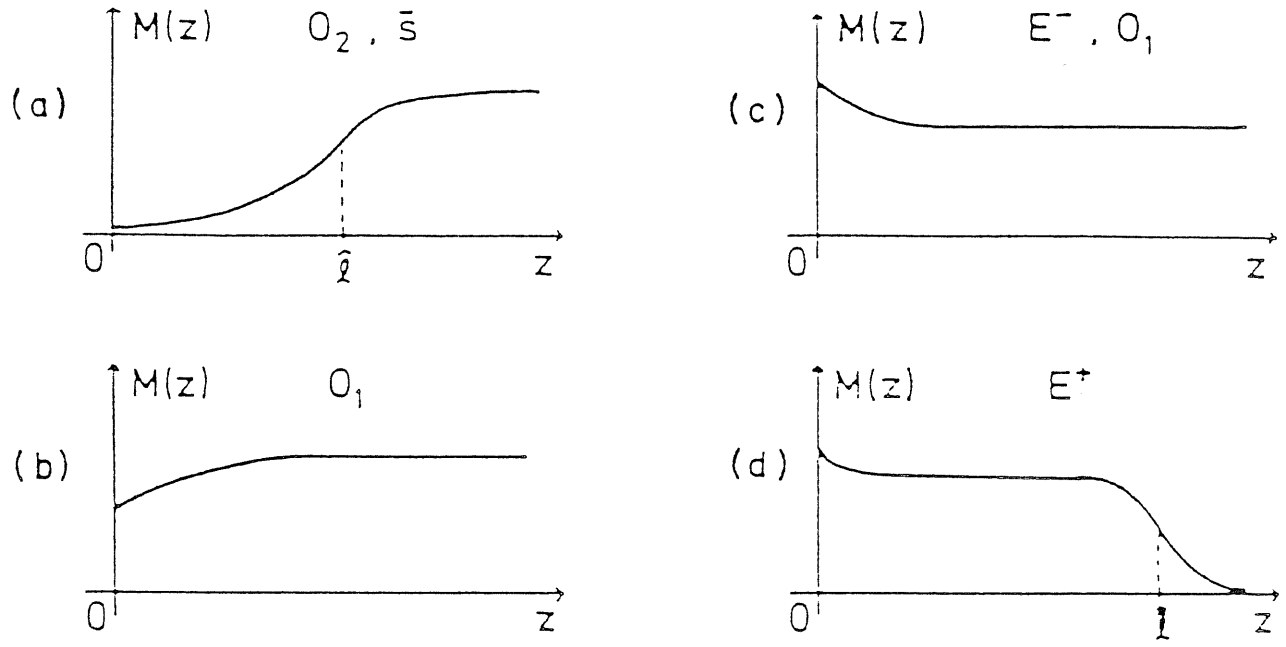

Figure 2.2: Generic shapes of the order parameter profile $M(z)$. We are interested in the O_2 profile.

transition (O_2); if one tries an exact treatment, it has been shown by Lipowsky *et al.*[13] that in bulk dimensionality $d = 3$ the MF logarithmic behaviour is recovered, whereas in bulk dimensionality $d = 2$ the divergence in the position of the interface is power-law, with an exponent $\beta_s = -\frac{1}{3}$.

The preceding discussion is limited to the case of a surface which perturbs the system with short range forces, here schematised with a δ-like interaction. However, long-ranged forces are also very important especially in the *surface melting* description.

Lipowsky ([14]) considered a Landau-Ginzburg-Wilson Hamiltonian in which the cost of the solid-liquid and of the liquid-vapour interfaces, together with the interaction between those, is considered. This Hamiltonian has the form:

$$H[z_{sl}, z_{lv}] = \int d^{d-1}x[\frac{\sigma_{sl}}{2}|\vec{\nabla} z_{sl}(x)|^2 + \frac{\sigma_{lv}}{2}|\vec{\nabla} z_{lv}(x)|^2 + U[z_{lv} - z_{sl}]], \tag{2.5}$$

where σ_{sl} and σ_{lv} are the interfacial free energies and z_{sl}, z_{sv} their d-th coordinates. Through a simple change of variables it is possible to write the expression (2.5) in function of the local interface width $l(x)$, where x is a $d-1$-dimensional vector. It can be shown that if the effective potential of interaction $U(l)$ between the two interfaces has an inverse power-law behaviour in addition of a linear term:

$$U(l) = \delta\mu l + \frac{1}{l^p}, \tag{2.6}$$

(here $\delta\mu$ is the difference in chemical potential between solid and liquid phase) and in mean-field approximation, the mean thickness of the wetting layer has a power-law divergence(exponent of $-\frac{1}{3}$) as the system approaches the critical point. Moreover, it has been

shown by Lipowsky [14] that this behaviour remains also when fluctuations in the local position of the interface are considered, whatever the value of the integer p in the (2.6). In particular, the case of bulk dimensionality 2 was deeply studied. The mean thickness $< l >$ of the wetting layer was found to diverge as $< l > \propto (\delta\mu)^{\beta_s}$: $\beta_s = -\frac{1}{1-p}$ in MF case and in the $p < 2$case, whereas $\beta = -\frac{1}{3}$ in the $p >= 2$ case.

The case of bulk dimensionality 2 has a connection with our physical system, *i.e.* the reconstructed stepped surface. In our case one could imagine an order parameter describing the reconstruction, or, better, a whole set of order parameters, i.e. the Fourier components of the surface density corresponding to the extra spots in the reciprocal lattice associated with the appearance of reconstruction. The reconstructed flat surface would then represent the ordered bulk, whereas the unreconstructed surface would be the disordered bulk phase. The presence of the step (an unidimensional surface) would then induce a disordered zone, leading to an interface between the different bidimensional structures.

According to Lipowsky's scheme, at the deconstruction temperature the length of the reconstructed zone should increase with temperature and diverge logarithmically or power-law at the critical point, depending on the forces between step and interface. In practice, one can establish the following correspondence between Lipowsky's theory and the reconstruction on a stepped surface:

bulk	$\longrightarrow$	Au stepped surface
surface	$\longrightarrow$	step
order parameter(s)	$\longrightarrow$	reconstruction diffraction spots
interface	$\longrightarrow$	interface btw. reconstructed-deconstructed zone
$< l >$	$\longrightarrow$	width of the reconstructed zone

The physical nature of the interactions between steps and interfaces is hard to determine. As shown in the preceding chapter, entropic, stress-induced and dipole-induced interactions between step have all the same d^{-2} behaviour. What about the interactions between steps and interfaces between reconstructed and unreconstructed zones? Is the form of this interaction really important in determining the critical properties of the wetting layer (in our case, the disordered zone around the step)?

The answer to the latter question is *no*; this can be seen from the preceding theoretical discussion: short-range and long-range forces give all, in $d = 2$, the same power-law divergence for the mean width of the wetting layer, with exponent $-\frac{1}{3}$. The answer to the former question cannot, at present, be given, although it would be important to give quantitative weight to this approach.

At this point it is necessary to point out some differences, which are of crucial importance in determining the faceting scenario. First of all, the terrace has a finite width; as long as the width of the reconstructed zone is smaller than the width of the terrace, an interface

between reconstructed and non-reconstructed zone takes place. In Lipowsky's approach, this corresponds to consider a system which is no longer semi-infinite, but has a finite width L and is delimited by two surfaces (the steps).

The main effect of L finite is a shift of the bulk coexistence curve to a lower temperature [15]. The thickness $\langle l \rangle$ of the disordered layer, if one considers the fluctuations in $d = 2$, behaves again as a $-\frac{1}{3}$ power law, but with a maximum value $L^{\frac{1}{3}}$, for large but finite L.

However, the interface is energetically unfavourable, due to the gradient term in Landau-Ginzburg expansion (see for example [13]). At a certain temperature, if the terrace is thicker than $\langle l \rangle$, the surface undergoes a phase separation, i.e. the faceting transformation. If, conversely, the terrace is narrower, corresponding to a more tilted vicinal, the unreconstructed zone at high temperatures invades the whole terrace, the interface disappears and the vicinal becomes stable.

This simple scenario is only an hypothesis of work; the only available experimental data concern the phase diagram which is consistent with this description. We decided to carry out a Molecular Dynamics simulation study in order to investigate the validity og such scenario. In spite of several unexpected difficulties, some light has been shed on the problem. In the next chapter we discuss the method, and present our preliminary results on the orientational behaviour of Au(100) and its vicinals at finite temperature.

3 MD simulations of Au(100) and vicinal surfaces

3.1 Introduction

From the experimental point of view, the (100) surface of Au is known to undergo a first order deconstruction transition from hexagonal order to disordered at 1170 K (*i.e.*, $0.88T_m$) [16, 17]. Abernathy *et al.*[18], using X-ray scattering, presented a detailed study about the orientational epitaxy of the hexagonal (low-temperature) phase both of gold and of platinum. The study reveals the coexistence of domains with slightly different orientation with respect to the substrate and to each other. The rotation angles vary in a continuous way for some domains and in an abrupt, first-order way for other domains. Such angles are, however, very small (of the order of 1°), and measurable only with very accurate x-ray scattering techniques. A corrugation of the surface is also observed which propagates several layers into the bulk and the hexagonal overlayer is shown to be incommensurate.

Conversely, above the transition temperature the peaks in x-ray reflectivity due to the hexagonal overlayer disappear, and the observed pattern is consistent with that of a disor-

dered surface with one or two melted layers.

The tool of classical Molecular Dynamics (MD) simulation appears very useful in verifying by the microscopic point of view such experimental results.

The 'glue potential' which I will briefly describe in next section, has been successfully applied to noble metals, and particularly to gold.

The (100),(111) and vicinal surfaces of gold were studied with molecular dynamics both at $T = 0$ [7] and at finite temperatures [19]; both reconstruction and faceting properties at low temperatures were predicted. and surface melting, together with non-melting induced faceting were found.

We have done a MD simulation study by heating slab-shaped samples from $T = 0$ up to $.92T_m$, where $T_m = 1355K$ is the 'simulation melting point' as determined in previous bulk simulations[20].

3.2 Glue force model and the molecular dynamics method

The failures of pairwise interaction models in describing bulk and surface properties of metals are well known (*e.g.* [20, 21]). To develop a realistic force model, it is necessary to keep into account the 'gluing' role of conduction electrons in a metal. The electronic environment in which each ion is situated plays a crucial role in determining the local energetics. different environments correspond to different effective forces between ions, requiring a many-body force model for a realistic description, particularly when undercoordinated atoms such as surface atoms are present. During the 80s several schemes based on the concept of a non-

linear energy dependence upon a local coordination variable were developed to simulate metals realistically. One of the most famous, successfully tested and simplest many-body Hamiltonians of this family was developed by Ercolessi, Parrinello and Tosatti. In this "glue model" the potential is made up of two parts and has the form [20]:

$$V = \frac{1}{2}\sum_{ij}\Phi(r_{ij}) + \sum_{i}U(n_i), \tag{3.1}$$

where r_{ij} is the distance between atoms i and j , and $n_i = \sum_j \rho(r_{ij})$ is a generalized coordination of the atom i, calculated as a sum of contributions by the neighbours. The two-body potential $\Phi(r)$, the "glue" function $U(n)$ and the function $\rho(r)$ are constructed empirically, by fitting physical properties of the material.

Standard molecular-dynamics (MD) has been used to investigate a variety of bulk and surface systems, using the glue force model introduced previously. By MD one can manipulate a system of N interacting particles to bring it to the desired thermodynamic state.

I used, as usual, as initial conditions regular arrays of points of opportune geometry, with suitably randomized small displacements and all zero-velocities. Starting from these initial conditions, the time evolution of the system is followed by numerical integration of the classical Newton's motion equations. If the system under study is ergodic, thermodynamic and statistical information can be extracted by time averaging over runs of adequate length.

The temperature of the system (a micro-canonical ensemble) is introduced as a scale for measuring the kinetic energy:

$$\frac{1}{2}\sum_i m_i \dot{r}_i^2 = \frac{3}{2} N k_B T(t) \tag{3.2}$$

MD can also be effectively used as an energy minimization tool, by removing kinetic energy from the system until the particles have reached an equilibrium position.

The problem in MD is to convert differential equations into a set of difference equations, which allow to go from time t to $t + \Delta t$ with a suitably chosen Δt. A typical Δt for gold is $.7\ 10^{-14} sec$. This can be done with several algorithms. In my calculations, it has been used a fifth-order predictor-corrector algorithm, which can be found in a report by Gear[22].

In particular, the glue potential accounts correctly for the stable structure of the (100) Au surface at low temperatures [23, 21, 24].

3.3 The (1 0 0) surface.

The flat (100) surface of gold constitutes a classic example of surface reconstruction of noble metals. Since the early electron diffraction studies [25], the surface layer structure of Au(100) is known to be nearly-triangular (see Fig. 3.1). Interaction of this dense top layer with the underlying unreconstructed crystal planes produces a large unit cell, more recently estimated to be close to (28×5) [26, 27, 28, 16, 17]. The fivefold periodicity is due to the stacking of six [011] rows on top of five rows in the second layer. The large periodicity in the orthogonal direction is the consequence of a small contraction along the [011] rows. The density increase with respect to a regular (100) crystal plane is about 24 percent. Theoretical investigations of this surface [23] indicated that this reconstruction is

driven by the tendency of surface atoms to increase packing, which in turn may be explained in terms of the surface electronic structure [29].

X-ray reflectivity measurements as a function of temperature [16, 17] show that the hexagonal diffraction spots disappear abruptly around $T_c \simeq 1170\,\mathrm{K}$ (i.e., $\sim 0.875\,T_m$ where T_m is the melting point). The transition has been characterized as a triangular-to-disordered, first-order phase transition [16, 17].

In this section we investigate the mechanisms of deconstruction of this surface, using the glue potential and molecular dynamics.

Our system was a (100) 16-layer slab containing about 14000 particles, with the first layer initially arranged in a nearly optimal triangular structure. Temperature was carefully raised from zero up to 1300 K, where the surface is (incompletely) melted [19]. From here the system was then slowly cooled in small steps of 10 K, with a very long annealing time of about 0.5 ns at each temperature.

Upon heating, the lateral density of the surface is seen to increase with increasing temperature, as shown in Fig. 3.2. This unusual behaviour is confirmed experimentally for both Au and Pt [17]. The temperature-driven density increase appears to be connected with the same packing tendency which causes the reconstruction at $T = 0$. When the surface layer contracts laterally going from square to triangular, it does so with an additional vertical *outward* relaxation over the second layer. The vertical expansion is easy to understand, since in fcc the interplanar spacing is 15% larger for (111) planes than for (100) planes, and the present situation [a (111) plane over a (100) plane] is intermediate. As temperature

rises, the outward relaxation undergoes a further, anomalously large anharmonic increase. This anomalous expansion is confirmed in our simulation, and its magnitude is in fairly good agreement with X-ray data [16, 17]. In correspondence with the vertical expansion, the first, triangular layer becomes less coupled to the second, and the interplanar contribution to surface coordination decreases very strongly. The additional in-plane contraction therefore takes place to compensate for this decrease with a corresponding in-plane increase, which is necessary to keep energy from growing excessively.

A second feature which we find in connection with the lateral increase is the formation of a large surface vacancy island, or "crater", one monolayer deep, clearly visible for example in Fig. 3.3, showing the surface just below T_c. These craters, also observed earlier by Bilalbegovič and Tosatti [19], appear at first to be a consequence of the increased lateral density and of MD particle conservation, although it is not excluded that they might represent equilibrium features. In any case a crater is a fairly localized feature, and its presence is therefore not too disturbing. Ignoring the crater region, we see in this figure the surface triangular reconstruction, its domain wall-like stripe features distorted, but not removed by thermal fluctuations.

To measure the degree of orientational order, we calculate the sixfold orientational order parameter [30] at each atomic site i:

$$O_{6i} = \frac{1}{N_i} \sum_j e^{6i\theta_{ij}} \tag{3.3}$$

where the sum is limited to the N_i in-plane first neighbours of i, and θ_{ij} is the angle formed by the ij bond, projected on the xy plane, with the x axis. $|O_{6i}|$ measures the degree of local

triangular order at the surface, while the phase measures the local lattice orientation. We then construct a long-range order parameter average $|\langle O_6 \rangle| = |\left\langle \frac{1}{N} \sum_i O_{6i} \right\rangle|$, where the sum on i is extended to all the N atoms at the surface and $\langle \ldots \rangle$ indicates averaging over many configurations; and its short-range counterpart, the average modulus $\langle |O_6| \rangle = \left\langle \frac{1}{N} \sum_i |O_{6i}| \right\rangle$. In order to select the surface atoms we used the same algorithm used by Celestini *et al.* [31].

Results for the profiles of order parameters parallel to the surface at $T = 1040\,\mathrm{K}$ are shown in Fig. 3.3(b). Away from the crater, we find a value for $|\langle O_6 \rangle|$ of about 0.5, characterizing the finite amount of long-range order at this temperature. While $|\langle O_6 \rangle|$ is depressed in the crater region, $\langle |O_6| \rangle$ is not, indicating that the crater bottom is again reconstructed (as seen also by the lateral density).

The situation changes abruptly above $\sim 1050\,\mathrm{K}$. Fig. 3.4 shows, for example, a picture of the surface at 1100 K. The stripes have now lost their connectivity, and the surface is disordered. This is confirmed by a value of $|\langle O_6 \rangle|$ of about 0.15, well below its value below T_c, and in fact compatible with zero for infinite size. It is important to note that only the long-range order parameter, $|\langle O_6 \rangle|$, has dropped whereas short-range order, as measured by $\langle |O_6| \rangle$, unaffected by phase disorder, remains high. Hence we can conclude, as is also clearly suggested by Fig. 3.4, that the mechanism of deconstruction is tied to the loss of coherence of locally triangularly ordered domains, with collapse of the one-dimensional stripes which divide them.

While this picture is rather appealing, there is a disturbing point. Ignoring the crater

regions, we find that the lateral surface density levels off, but does not decrease across and above $T_c = 1050\,\mathrm{K}$ (Fig. 3.5). This is in apparent contrast with a fit of the specular X-ray intensity, indicating a drop of lateral density, from 1.33 below T_c to 0.96 above T_c[16. 17]. The reason for this disagreement is presently unclear. One possible danger is that in true grand canonical equilibrium, the surface structure and density might behave differently from our simulated, strictly canonical system.

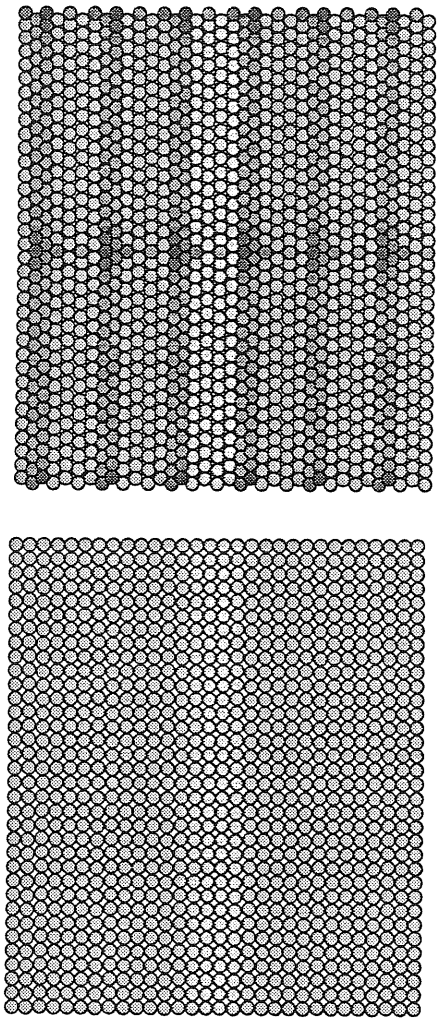

Figure 3.1: The reconstructed (100) surface at $T = 0$, and the corresponding bulk layer.

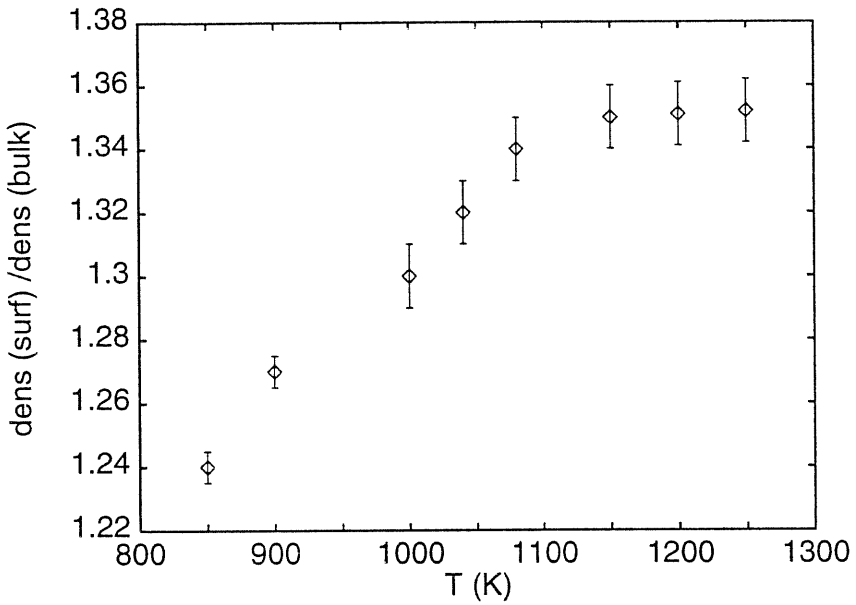

Figure 3.2: Lateral surface density of Au(100) from MD simulations as a function of temperature. Note the steady increase, and a leveling off around the glue model deconstruction temperature $T_c = 1050\,\mathrm{K}$ (experimental $T_c = 1170\,\mathrm{K}$).

3.4 The (53 1 1) vicinal and the step-reconstruction interaction.

In the previous chapters we investigated the possible role played by a step in the reconstruction-deconstruction scenario.

The simulation of a surface with a single step appears to be a very tricky job, due to the mismatching of the periodic boundary conditions; to obtain a slab which shows the correct structure when the finite sample is replicated by periodic boundary conditions along the xy plane it is necessary to introduce, on the (100) surface of an fcc crystal, an even number of monoatomic steps.

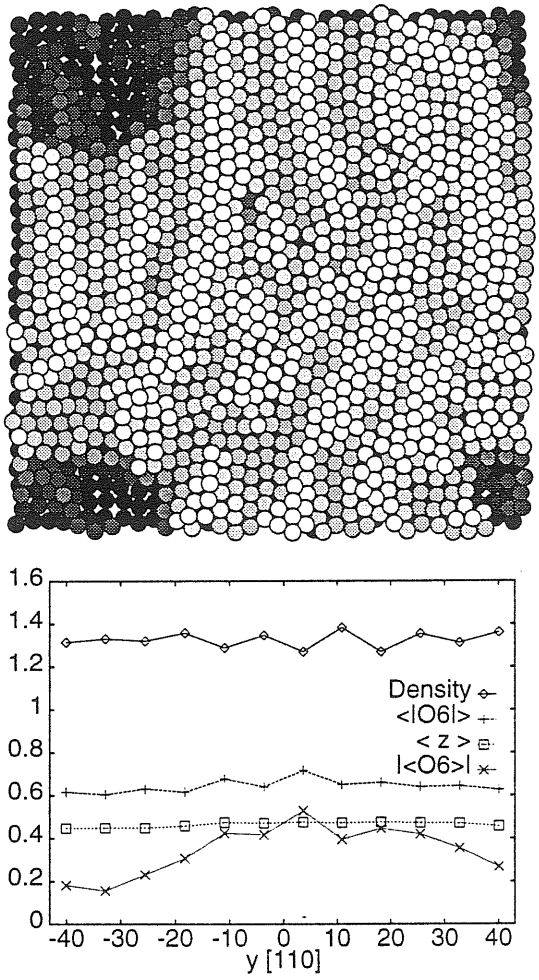

Figure 3.3: Simulation results for Au(100) at 1040 K (just below T_c) (a) Top view of a configuration. The grey scale represents the z coordinate of atoms; lighter zones are higher. The reconstruction is visible mainly through the striped domain-walls. The "crater" discussed in the text is visible at the four corners (a single crater, seen with periodic boundary conditions). (b) Surface density (relative to that of a bulk (100) plane), long-range and short-range order parameters, and height profile. Quantities shown as a function of the y coordinate in the surface plane. after averaging along on the x coordinate. Note the depression of long-range order and of height, but not of short-range order and of density, caused by the crater.

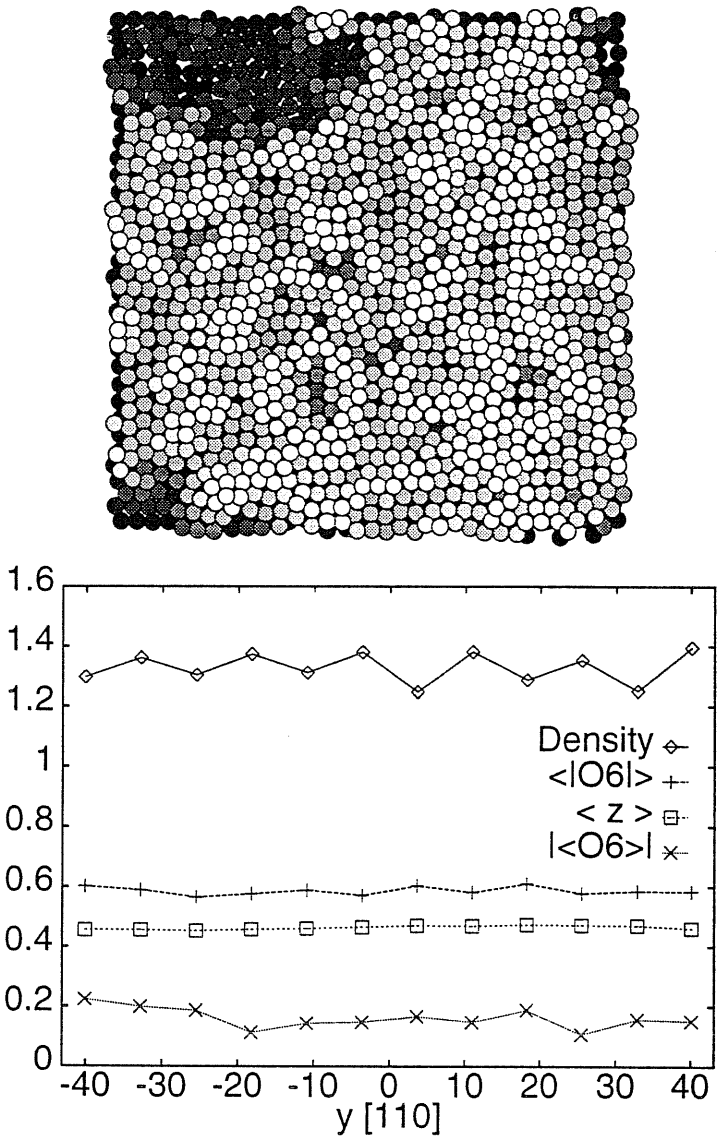

Figure 3.4: Simulation results for Au(100) at 1100 K (just above T_c). Same notations and conventions as in Fig. 3.3. The domain wall stripe order is now spoiled. The long-range order parameter has dropped, indicating deconstruction. Short-range order and high density remain, suggesting that deconstruction is due to loss of long-range phase coherence of the triangular overlayer.

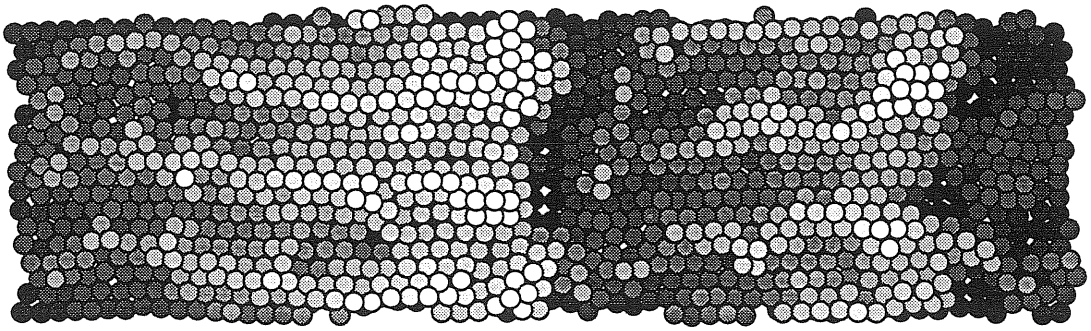

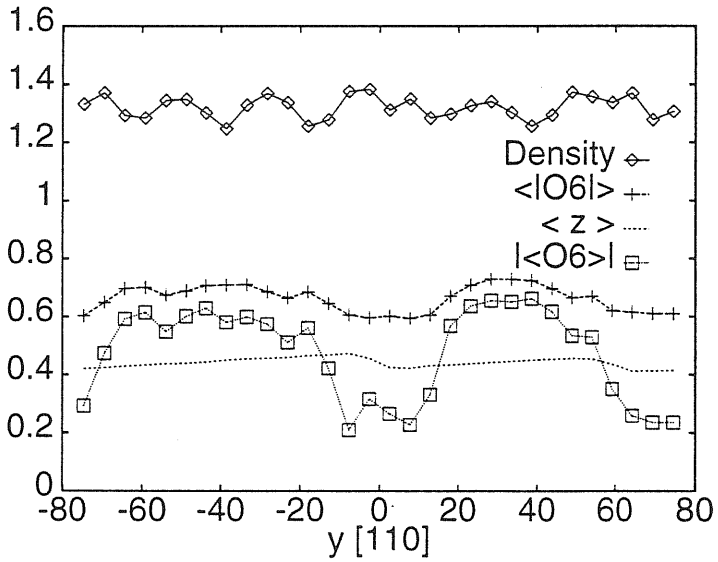

Figure 3.5: Simulation results for a surface with steps, Au(53,1,1) at 970 K. Same notations and conventions as in previous figures. One of the two steps has retreated, thus increasing the lateral density. Note that orientational order is stronger on the rim of a step, and is depressed at the foot of a step. On the rim, stripes orient preferentially normal to the steps, as also seen experimentally.

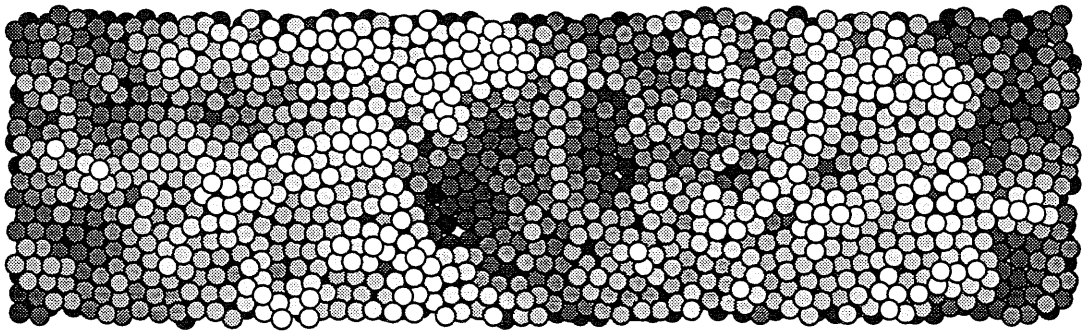

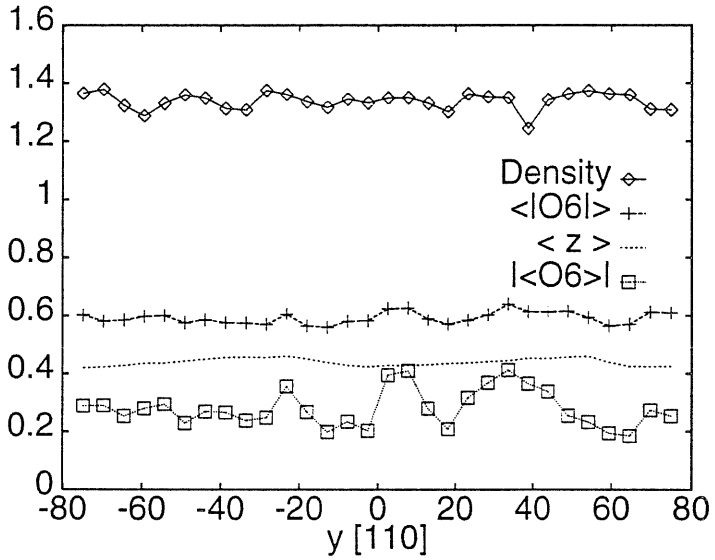

Figure 3.6: Simulation results for a surface with steps, Au(53.1.1) at 1250 K. Same notations and conventions as in previous figures. There is no more order, but short-range order and lateral density remain high.

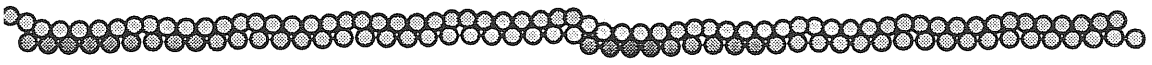

Figure 3.7: The reconstructed (53,1,1) surface at $T = 300K$ (side view). Note the 5 extra lines on each terrace.

However, if the terraces are wide enough, it may be assumed that the steps don't interact but weakly; in practice, one can study the effect of a single step on the terraces which it separates. For this reason, we investigated a surface (m 1 1) with m very high, i.e. the $m = 53$ case. The choice of $m = 53$ was intentional: it was shown that the width of a terrace is in this case *ideal* to accommodate 5 extra rows of atoms , giving rise to a structure with 5 reconstruction units on each terrace. The orientation of this surface is therefore energetically stable(magic vicinal) [7]. The sample was a 12105 particles slab, with 3 bulk rows blocked, and the surface was made up of 2 steps and 2 wide, reconstructed terraces. The cycle of simulation was similar to the one followed in the flat surface case.

The results obtained from this surface can be summarized as follows:

- The step actually represents a repulsive barrier for the reconstruction. We will see below that there is a zone of the surface where the $O6$ order parameter is lower, even at temperatures at which the reconstruction should be strong, and this zone is actually

near the step.

- The surface shows domains with different hexagonal orientation, and this is consistent with experimental works [18].

- There is a zone where there is neither hexagonal nor square order, even at relatively low temperatures, indicating that the non-reconstructed phase at low temperature is not simple to describe.

3.4.1 Example of evolution at 970 K and at 1250 K

Fig. 3.5 shows the results obtained after a long annealing at a temperature below T_c. We find that starting with terraces of equal width, and an initial surface density 1.24, one of the steps retreated visibly (the other appears to be pinned to the corresponding rigid bottom step, probably due to insufficient thickness). The surface density is roughly uniform, while the orientational order parameter is greatly reduced near the step. The stripes preferred orientation is orthogonal to the step. The presence of the step represents a perturbation to the orientational order parameter.

By heating the same system above T_c, the orientational order parameter drops (Fig. 3.6), but again the density shows no decrease. The disagreement with the X-ray data fit therefore remains. No final word can be said, however: although the value of 53 for the first Miller index of the vicinal is quite high, the interaction between the steps can hardly be ignored. Moreover, the width of the terrace is again too small for it to reproduce the physics of a flat (100) surface; it seems necessary a grand-canonical treatment of the problem, to allow the

system to increase or decrease its density without changing its features introducing holes or shortening the terraces. Work in this direction is presently in progress.

3.5 Other vicinal surfaces and the (17,1,1) surface.

In this section I will describe preliminary results concerning faceting of other, more tilted, vicinal surfaces. The choice, and consequently the compromise, to be made is between big samples, with large times of equilibration but a final state closer to the experimental one, and small samples with smaller times of equilibration but a final state to be interpreted as a *"finite size equilibrium state"*. We started with big samples with a very large surface and observed that the times of equilibration of such samples was so high that many months of computer time would have been necessary to obtain a non-noisy signal. In particular, a source of problem was originated by the fluctuation of the steps in the x direction (parallel to the step itself).

The next attempt was therefore to reduce considerably the size of the sample, especially in the x direction. In this way we could observe the first signals of faceting with more clarity, and focus on the more interesting temperatures and orientation.

The same path of simulation was followed for a large number of vicinals, *i.e.* (M 1 1) with M odd and ranging from 11 to 35.

A typical sample was made up of two steps, and very thin in the x direction.

The preliminary results obtained from these 'wide spectrum' simulations can be summarized as follows:

- Clear, stable faceting has been observed in a temperature range between 1000 and $1080K$. This is consistent with the experimental picture described by Watson[32].
- A totally different behaviour was observed at lower temperatures. This fact is consistent again with the experimental picture and with the idea that at low temperatures 'magic vicinals' appear, this situation being very stable varying the temperature.
- The mechanism of 'bunching' of the steps was efficiently monitored and measured. leading to a complicated picture of the interaction between the steps.
- The angle of faceting, which is presumed to be variable with temperature according to the (1.6) is very difficult to measure with such a precision to confirm or disregard this experimental fact and theoretical prediction.

3.5.1 Evolution of the interaction between the steps

In this section, I would like to show two examples of the steps pairing mechanism originating the phenomenon of faceting. In Fig. 3.8 the starting configuration is a surface with four equally spaced steps; the figure shows a side view of the surface and few sublayers, doubled in the direction perpendicular to the step to simplify the observation. As the simulation ($T = 1080K$) proceeds, the formerly separated steps begin to join together and at the end a 'hill-and-valley' structure is recognizable.

In Fig. 3.9 a similar evolution path is described at $T = 1050$. The starting configuration is a couple of paired steps (doubled in the x direction in the figure) which again tend to join together. In particular, after ~ 5 $nsec$ (nineth frame in the figure) a clear bunching of

all the steps is observed, but the small dimensions of the sample do not permit to conclude anything about the angle of faceting. It seems remarkable, however, that this hill and valley structure has been observed on a wide range of vicinals, encouraging further work in this direction.

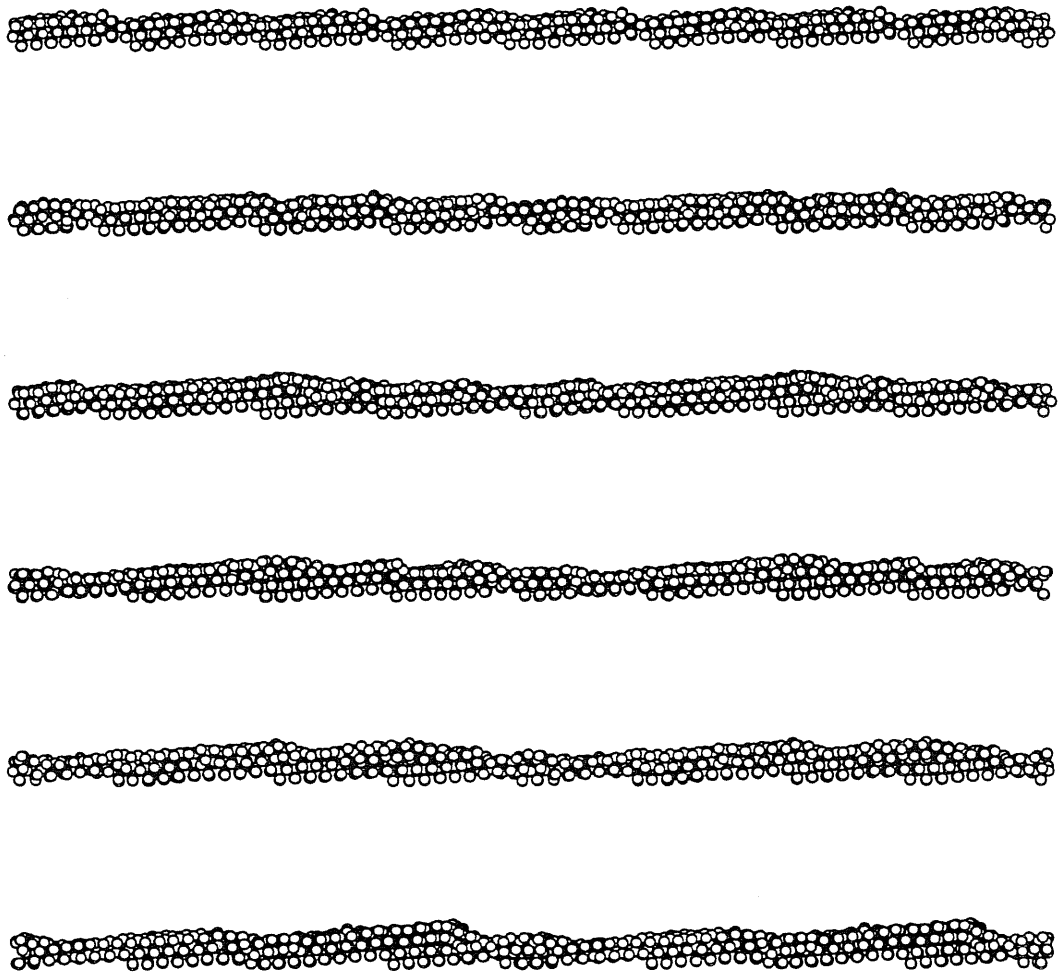

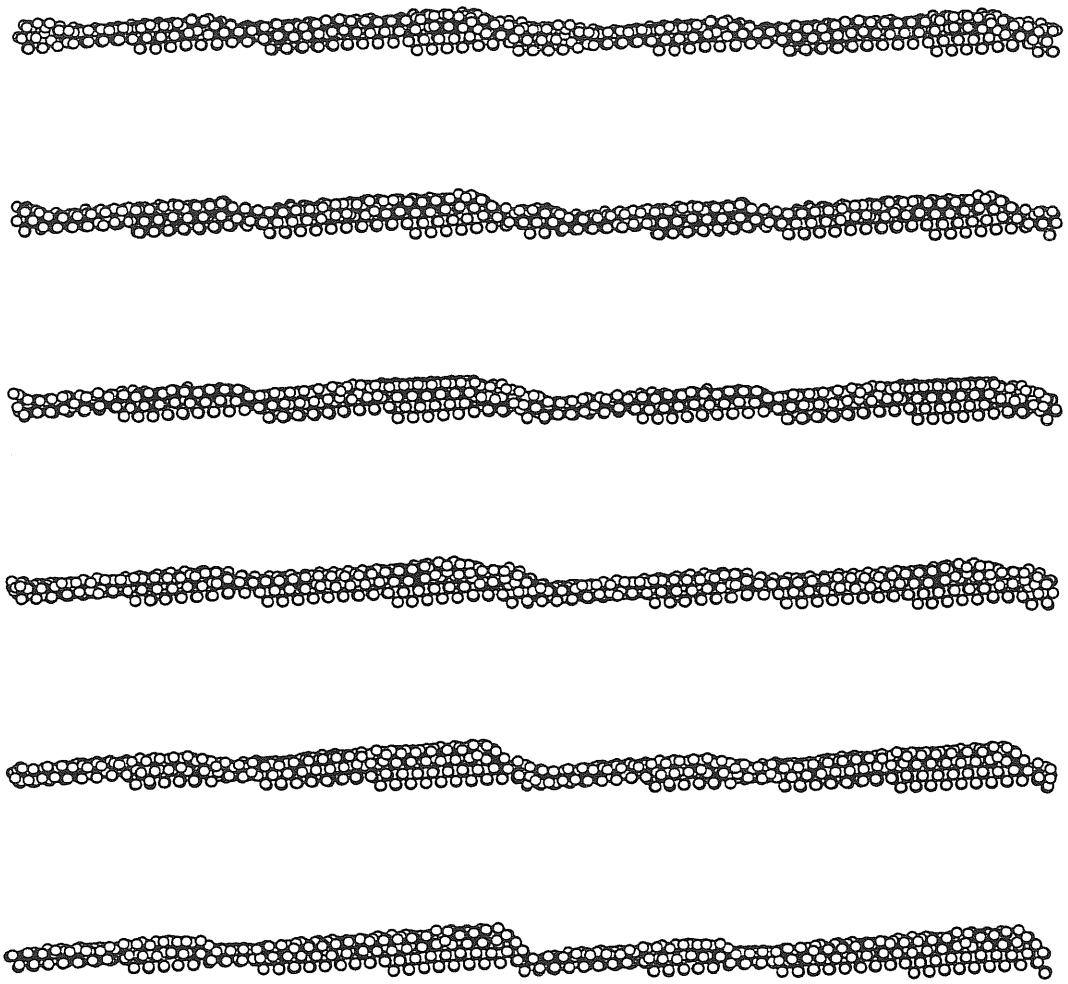

Figure 3.8: Time evolution of the surface (T=1080) (side view). Note the attraction between the steps leading to faceting (Δt in the first 6 frames: .7 *ns*, in the others: .35 *ns*. 2 MD boxes are shown.

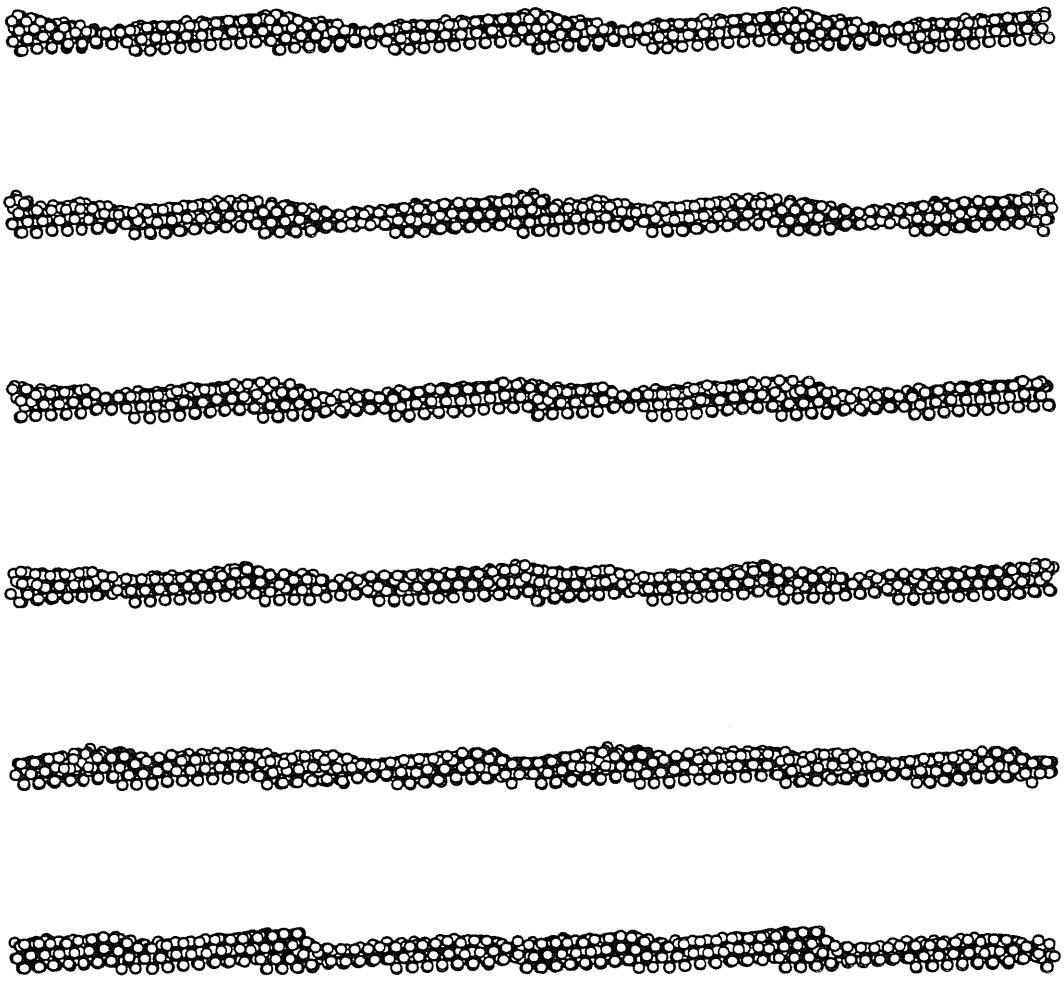

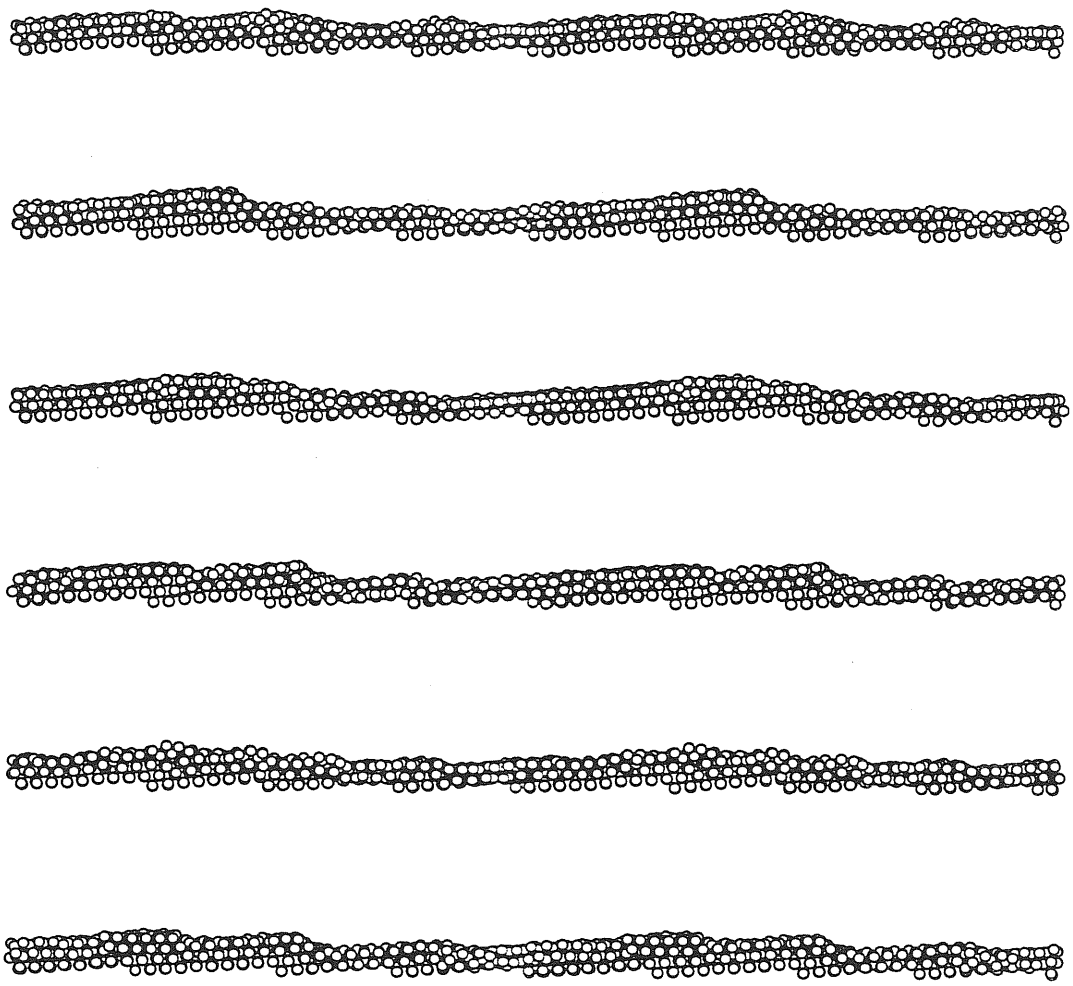

Figure 3.9: Time evolution of the surface(T=1050) (side view). Note the attraction between the steps leading to faceting (Δt in the first 6 frames: .7 *ns*, in the others: .35 *ns*. 2 MD boxes are shown.

Conclusions and Perspectives

In order to understand thoroughly, from a microscopical point of view, the mechanisms leading to faceting of vicinal surfaces, a study of the deconstruction of flat Au(100) and of the role played by steps on its vicinals has been carried out during this work. We have found that the lateral surface density increases with increasing temperature and that the transition takes place due to loss of long-range coherence of locally triangularly ordered domains. Simulation problems arise due to the change of surface density, which is hampered by the particle conserving algorithm. In particular, there is a disagreement with X-ray specular reflectivity fits which predict a sudden decrease of the density at the deconstruction temperature [16, 17]. These fits, however, have been done using a model with completely occupied layers; such a geometry is only one of the possible equilibrium states of a flat surface, and our 'holes' appearing during the simulation cannot be definitely interpreted neither as canonical artifacts to increase the lateral density, nor as equilibrium features. At present we are developing new techniques, such as grand-canonical Monte Carlo simulations, to answer this question.

When steps are added to help solve this problem, an interesting interplay is found

between steps and reconstruction. The step acts as a repulsive barrier for the reconstruction: at low temperatures, the sixfold order parameter remains high on the terrace, whereas it is depressed in a zone around the step; therefore, an interface between deconstructed and reconstructed zone appears, confirming phenomenological descriptions of the faceting phase separation described in the second Chapter. Moreover, the pairing of few steps leading to faceting, observed during the MD simulations, suggests further efforts in this direction, although, at the present state of work, it seems difficult to reach a quantitative evaluation of the angle of faceting by applying the MD tool to such small samples.

Acknowledgements

First of all, I would like to thank Chiara for her patience and lovely assistance. Moreover, I thank my parents for their moral and material support and all the friends in Sissa: my mates Marco, Claudio, Alice, Carlo, Orion, Nicola, Claudia, Franz, Paggio and Barbara and all the people who contributed to creating an appealing and warm atmosphere during all this period.

In particular, I wish to thank explicitly Franz di Tolla for his help in solving physical and personal problems; Marco and Claudio with whom I share the apartment in Trieste together with a wonderful friendship; Alice, with whom I share only the wonderful friendship. Last, but of course not at all least, I thank my supervisors Erio Tosatti and Furio Ercolessi, for the continuous help and encouragement during all this year of work.

Bibliography

[1] G.Wulff, Z.Krist. **34**(1901)449.

[2] C.Herring, Phys.Rev.**82**(1951)87.

[3] E.D. Williams, Surf.Sci. **299,300**(1994)502.

[4] J.S.Ozcomert, W.W.Pai, N.C.Bartelt and J.E. Reutt-Robey, Phys.Rev.Lett. **72**(1994)258.

[5] S.Song and S.G.J.Mochrie, Phys.Rev.Lett **73**(1994)995.

[6] G.Bilalbegovič F.Ercolessi and E.Tosatti. Europhys. Lett. **17**(1992)333.

[7] A.Bartolini, *Ph.D. Thesis* and A.Bartolini, F.Ercolessi and E.Tosatti, Phys.Rev.Lett. **63**(1989)872.

[8] G.M.Watson, Doon Gibbs, D.M.Zehner. M.Yoon and S.G.J.Mochrie, Phys.Rev.Lett **71**(1993)3166.

[9] G.M.Watson *et al.*, Bull. Am. Phys. Soc. (1995), unpublished research.

[10] Y.Samson *et al.*, Surf.Sci.Lett **315**(1994)L969.

[11] R.J.Phaneuf and E.D.Williams, Phys.Rev.Lett. **58**(1987)2563.

[12] R.Lipowsky and W.Speth, Phys. Rev. B **28**(1983)3983.

[13] R.Lipowsky, D.M.Kroll and R.K.P.Zia, Phys.Rev.B**27**(1983)4499.

[14] R.Lipowsky, Phys. Rev. B **32**(1985)1731.

[15] R.Lipowsky and G.Gompper, Phys.Rev.B **29**(1984)5213.

[16] S. G. J. Mochrie, D. M. Zehner, B. M. Ocko, and D. Gibbs, Phys. Rev. Lett. **64** (1990) 2925; D. Gibbs, B. M. Ocko, D. M. Zehner, and S. G. J. Mochrie, Phys. Rev. B **42** (1990) 7330; B. M. Ocko, D. Gibbs. K. G. Huang, D. M. Zehner, and S. G. J. Mochrie. Phys. Rev. B **44** (1991) 6429; D. L. Abernathy, S. G. J. Mochrie, D. M. Zehner, G. Grübel, and D. Gibbs, Phys. Rev. B **45** (1992) 9272.

[17] D. L. Abernathy, D. Gibbs, G. Grübel, K. G. Huang, S. G. J. Mochrie, A. R. Sandy, and D. M. Zehner, Surf. Sci. **283** (1993) 260.

[18] D.L.Abernathy, S.G.J.Mochrie, D.M.Zehner, G.Grübel and Doon Gibbs, Phys.Rev.B **B45**(1992)9272.

[19] G.Bilalbegović and E.Tosatti, Phys. Rev. B **48**(1993)11240.

[20] F.Ercolessi, M.Parrinello and E.Tosatti, Philos.Mag.A **58**(1988)213.

[21] E. Tosatti and F. Ercolessi, Modern Phys. Lett. B **5** (1991) 413.

[22] C.W. Gear, ANL report 7126, Argonne National Laboratory, *Numerical Initial value Problems in Ordinary Differential Equations* (Pretice Hall, Englewood Cliffs, N.J. 1971).

[23] F. Ercolessi, E. Tosatti, and M. Parrinello, Phys.Rev.Lett **57** (1986) 719; F. Ercolessi, M. Parrinello, and E. Tosatti, Surf. Sci. **177** (1986) 314.

[24] A. Bartolini, F. Ercolessi, E. Tosatti, Phys. Rev. Lett. **63** (1989) 872.

[25] S. Hagstrom, H. B. Lyon, and G. A. Somorjai, Phys. Rev. Lett. **15** (1965) 491; D. G. Fedak and N. A. Gjostein, Phys. Rev. Lett. **16** (1966) 171; P. W. Palmberg and T. N. Rhodin, Phys. Rev. **161** (1967) 586.

[26] G. Binnig, H. Rohrer, Ch. Gerber, and E. Stoll, Surf. Sci. **144** (1984) 321.

[27] K. Yamazaki, K. Takayanagi, Y. Tanishiro, and K. Yagi, Surf. Sci. **199** (1988) 595.

[28] Y. F. Liew and G. C. Wang, Surf. Sci. **227** (1990) 190.

[29] J. F. Annett and J. E. Inglesfield, J. Phys.: Cond. Matt. **1** (1989) 3645; N. Takeuchi, C. T. Chan, and K. M. Ho, Phys. Rev. Lett. **63** (1989) 1273; V. Fiorentini, M. Methfessel, and M. Scheffler, Phys. Rev. Lett. **71** (1993) 1051.

[30] See, e.g., *Bond-orientational order in condensed matter systems*, K. Strandburg (Ed.), Springer, New York, 1992; K. Strandburg, Rev. Mod. Phys. **60**, 161 (1988).

[31] F. Celestini, F. Ercolessi and E. Tosatti, to be published.

[32] G.Watson, APS meeting 1995.